

Rapid optimization of working parameters of microwave-driven multi-level qubits for minimal gate leakage

Zhongyuan Zhou^{1,2}, Shih-I Chu¹, and Siyuan Han²

¹*Department of Chemistry, University of Kansas, Lawrence, KS 66045*

²*Department of Physics and Astronomy, University of Kansas, Lawrence, KS 66045*

(Received: June 29, 2005)

Abstract

We propose an effective method to optimize the working parameters (WPs) of microwave-driven quantum logical gates implemented with multi-level physical qubits. We show that by treating transitions between each pair of levels independently, intrinsic gate errors due primarily to population leakage to undesired states can be estimated accurately from spectroscopic properties of the qubits and minimized by choosing appropriate WPs. The validity and efficiency of the approach are demonstrated by applying it to optimize the WPs of two coupled rf SQUID flux qubits for controlled-NOT (CNOT) operation. The result of this independent transition approximation (ITA) is in good agreement with that of dynamic method (DM). Furthermore, the ratio of the speed of ITA to that of DM scales exponentially as 2^n when the number of qubits n increases.

PACS numbers: 03.67.Lx, 85.25.Dq, 89.70.+c

A practical quantum computer would be comprised of a large number of coupled qubits and the coupled qubits must be kept in high-degree quantum coherence states for sufficiently long time. During the past decade, significant progress has been made on physical implementation of quantum computation. High-degree quantum coherence has been demonstrated experimentally in systems such as trapped ions [1, 2], nuclear spins [3, 4], atoms in optical resonators [5], and photons in microwave cavities [6]. However, it seems quite difficult to realize a large number of coupled qubits using these systems. Meanwhile, solid-state qubits are of particular interest because of their advantages of large-scale integration, flexibility in design, and easy connection to conventional electronic circuits [7]. Of those, qubits based on superconducting devices have recently attracted much attention [8] as manipulation of quantum coherent states being successfully demonstrated in a variety of single qubits [9, 10, 11, 12, 13] and coupled two-qubit systems [14, 15, 16, 17, 18].

However, the solid-state qubits demonstrated in experiments so far all have relatively short coherence time and high probability of gate errors [9, 10, 11, 12, 13, 14, 15, 17]. One of the causes of these problems is extrinsic gate error arising from interaction between the environment and qubits resulting in decoherence, such as dephasing and relaxation [8]. Another cause is intrinsic gate error resulting from population leakage to undesired states due to the typical multi-level structures of solid-state qubits [19, 20]. The intrinsic gate error is crucial since it not only contributes to additional decoherence but also determines the ultimate performance of the quantum gates and cannot be eliminated by reducing the environment caused decoherence.

The leakage of a gate can be characterized quantitatively by summing up the maximum transition probabilities to all undesired states of a multi-level qubit [19, 20]. It depends strongly on energy level structure and transition matrix elements, i.e., spectroscopic properties of the

multi-level qubit determined completely by device parameters (DPs) and external control parameters of the qubit which we call working parameters (WPs) for simplicity. For instance, inductance (capacitance) of the superconducting flux (charge) qubit is a DP while external flux (gate voltage) is a WP. For the multi-level qubit with given DPs, the gate leakage is sensitive to their WPs and thus can be minimized by the use of appropriate WPs.

Conventionally, the leakage is calculated from transition probabilities to all undesired states by numerically solving the time-dependent Schrödinger equation (TDSE) [20, 21]. However, this kind of dynamic method (DM) not only needs complicated numerical algorithms but also a large amount of computational resources. For instance, optimizing the WPs of a many-qubit network needed for a practical quantum computer using DM may only be possible with *ad hoc* powerful quantum computers in the future. Thus a much faster approach is highly desirable.

In this Letter, we propose a very fast method to minimize the leakage of microwave-driven quantum logical gates by choosing appropriate WPs in a system of multi-level qubits with their DPs given *in prior*. We consider the case of weak microwave fields only since strong fields usually cause many additional types of intrinsic gate errors and thus should be avoided in general [20]. Our method is based on an independent transition approximation (ITA) in which transitions in multi-level qubits are treated independently. The leakage is estimated using the spectroscopic properties obtained by solving the eigenvalue equation of and minimized by optimizing the WPs of the qubits. The method is applied to minimize leakage of controlled-NOT (CNOT) gate implemented with coupled rf superconducting quantum interference device (SQUID) flux qubits. The result is in good agreement with that obtained from DM. More importantly, the ITA is scalable as the number of qubit n increases because the ratio of the speed of ITA to that of DM scales exponentially as 2^n .

A microwave-driven gate is realized via coherent transitions between the computational states of qubits interacting with microwave fields. In general, correlation and interference between transitions cannot be ignored and transition probability can only be computed accurately by solving TDSE. However, in weak fields, which is the case considered here, only the transitions between levels with which the microwave field is resonant or nearly resonant are significant. For a given level, if the level spacings between it and all other levels are sufficiently different, the correlation and interference between the transitions from this level have negligible effect. Hence, each transition is expected to take place independently and the two levels involved can thus be treated as if they are isolated from the others. For each of the two-level subsystems interacting with a rectangular pulse, the transition probability can be approximated by an analytical expression using the rotating-wave approximation (RWA). Assuming the rectangular pulse is $\epsilon(t) = \epsilon_0 \cos(\omega t)$, the interaction between the qubit and the pulse is then $V(t) = -\mu \cdot \epsilon(t)$, where ϵ_0 and ω are the amplitude and frequency of the pulse and μ is the dipole moment operator of the qubit. The maximum transition probability from state i to j in an N -photon process, \mathcal{P}_{ij} , is [22]

$$\mathcal{P}_{ij} = \Omega_{ij}^2 / (\mathcal{D}_{ij}^2 + \Omega_{ij}^2), \quad (1)$$

where, $\Omega_{ij} = 2\mu_{ij} \cdot \epsilon_0 N J_N(y_{ij})/y_{ij}$ is the Rabi frequency for the N -photon resonance, $\mathcal{D}_{ij} = \Delta E_{ij}/\hbar - N\omega$ is the detuning, $\mu_{ij} = \langle i | \mu | j \rangle$ is the dipole transition matrix element, $\Delta E_{ij} = |E_j - E_i|$ is the level spacing between the states i and j , J_N is the Bessel function of integer order N , and $y_{ij} = \mathbf{d}_{ij} \cdot \epsilon_0 / \hbar \omega$ with $\mathbf{d}_{ij} = \mu_{jj} - \mu_{ii}$. Note that \mathcal{P}_{ij} , Ω_{ij} , and \mathcal{D}_{ij} depend on the number of photons N . In weak fields characterized by $\Omega_{ij} \ll \omega$ only transitions with small N are important. Since the leakage is calculated from the maximum transition probabilities which are independent of pulse shape in weak fields [23] the optimized WPs obtained using rectangular pulse are also valid for other pulse shapes.

For the microwave-driven gate considered here, the microwave is resonant with a pair of computational states. According to Eq. (1), the leakage is suppressed if $\mathcal{D}_{ij} \gg \Omega_{ij}$ holds for all unintended transitions. This condition may be satisfied by using sufficiently weak fields and/or qubits with proper spectroscopic properties. However, the use of exceedingly weak fields will make the gate very slow. Even so the unintended transitions will still cause large leakage at or near resonance where $\mathcal{D}_{ij} \simeq 0$ and $\mathcal{P}_{ij} \simeq 1$ regardless of intensity of the fields. Thus the leakage can be greatly reduced by setting the level spacings of the qubits substantially detuned from the microwave frequency and/or the dipole transition matrix elements sufficiently small for all unintended transitions.

To investigate the leakage in a multi-level qubit, we study what happens when the microwave acts on each of the computational states, which we call a component of the gate. For an n -bit gate, there are $M = 2^n$ com-

ponents. The leakage of the i th component is defined as $\eta_i = \sum_k P_{ik}$, where P_{ik} is the maximum probability of occupying an undesired state k through all possible multi-photon transitions and the sum is over all the undesired states including all non-computational states as well as those computational states to which no transition is intended. The leakage of the n -bit gate, η , is then defined as $\eta = \max(\eta_1, \eta_2, \dots, \eta_M)$ which is a function of the ν WPs q_1, q_2, \dots , and q_ν . The set of WPs, $q_1^{\text{opt}}, q_2^{\text{opt}}, \dots$, and q_ν^{opt} is obtained by minimizing the leakage of gate, namely, $\eta(q_1^{\text{opt}}, q_2^{\text{opt}}, \dots, q_\nu^{\text{opt}}) \equiv \min[\eta(q_1, q_2, \dots, q_\nu)]$.

As an example, we apply ITA to optimize the WPs of coupled rf SQUID flux qubits for CNOT gate. Each rf SQUID consists of a superconducting loop of inductance L interrupted by a Josephson tunnel junction characterized by its critical current I_c and shunt capacitance C [24]. A flux-biased rf SQUID with total magnetic flux Φ enclosed in the loop is analogous to a "flux" particle of mass $m = C\Phi_0^2$, where $\Phi_0 = h/2e$ is the flux quantum. The Hamiltonian is $h(x) = p^2/2m + m\omega_{LC}^2(x - x_e)^2/2 - E_J \cos(2\pi x)$. Here, $x = \Phi/\Phi_0$ is the canonical coordinate of the "flux" particle, $p = -i\hbar\partial/\partial x$ is the canonical momentum conjugate to x , $E_J = \hbar I_c/2e = m\omega_{LC}^2\beta_L/4\pi^2$ is the Josephson coupling energy, $\beta_L = 2\pi LI_c/\Phi_0$ is the potential shape parameter, $\omega_{LC} = 1/\sqrt{LC}$ is the characteristic frequency of the SQUID, and $x_e = \Phi_e/\Phi_0$ is the normalized external flux.

The coupled rf SQUID qubits comprise two rf SQUID qubits: a control qubit and a target qubit coupled via their mutual inductance M [7, 25]. For simplicity, we assume that the two SQUIDs are identical: $C_i = C$, $L_i = L$, and $I_{ci} = I_c$ for $i = 1$ and 2 . The Hamiltonian of the coupled SQUID qubits is $H(x_1, x_2) = h(x_1) + h(x_2) + h_{12}(x_1, x_2)$, where x_i , x_{ei} , and $h(x_i)$ ($i = 1$ and 2) are the canonical coordinate, normalized external flux, and Hamiltonian of the i th single SQUID qubit and h_{12} is the interaction between the qubits given by $h_{12}(x_1, x_2) = m\omega_{LC}^2\kappa(x_1 - x_{e1})(x_2 - x_{e2})$. Here, $\kappa = M/L$ is the coupling constant. Note that each SQUID qubit is a multi-level system. The eigenstate $|n\rangle$ and eigenenergy E_n of the coupled qubits are computed by numerically solving the eigenvalue equation of $H(x_1, x_2)$ using the two-dimensional Fourier-grid Hamiltonian method [26]. They are functions of the WPs x_{e1} , x_{e2} , and κ for given device parameters L , C , and I_c [27, 28]. For weak coupling $\kappa \ll 1$, the eigenstate of the coupled qubits, denoted by $|n\rangle = |ij\rangle$, can be well approximated by the product of the control qubit's state $|i\rangle$ and the target qubit's state $|j\rangle$, $|n\rangle = |i\rangle|j\rangle$. When biased at $x_{e1}, x_{e2} \approx 1/2$ the potential of coupled SQUID qubits have four wells [7, 25]. The lowest eigenstates in each of the four wells, denoted as $|1\rangle = |00\rangle$, $|2\rangle = |01\rangle$, $|3\rangle = |10\rangle$, and $|4\rangle = |11\rangle$, are used as the computational states of the coupled SQUID qubits. For SQUIDs with $L = 100$ pH, $C = 40$ fF, and $\beta_L = 1.2$, the energy levels and level spacings versus x_{e2} and κ are plotted in Fig. 1(a)–(d), respectively. It is shown that both the

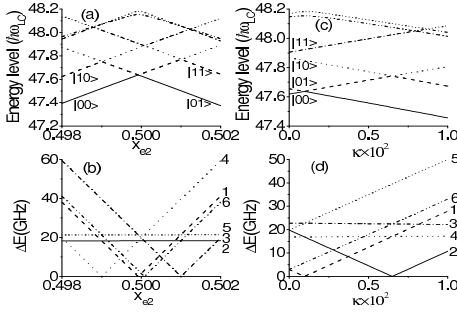


FIG. 1: Energy levels and level spacings of the coupled rf SQUID flux qubits. (a) the energy levels and (b) the level spacings vs. x_{e2} for $x_{e1} = 0.499$ and $\kappa = 5 \times 10^{-4}$, (c) the energy levels and (d) the level spacings vs. κ for $x_{e1} = 0.499$ and $x_{e2} = 0.49985$. The lines 1 to 6 in (b) and (d) represent the level spacings ΔE_{12} , ΔE_{13} , ΔE_{14} , ΔE_{23} , ΔE_{24} , and ΔE_{34} , respectively.

energy levels and level spacings are sensitive to the WPs x_{e2} and κ . When $x_{e2} < 0.49877$ or $x_{e2} > 0.50123$ in Fig. 1(a) or $\kappa > 7.5 \times 10^{-3}$ in Fig. 1(c) the energy level structures become quite complicated. Fig. 1(b) and Fig. 1(d) also show that in certain regions of the WP space the level spacings become crowded, meaning that they are degenerate or nearly degenerate, which may result in significant intrinsic gate errors.

Controlled two-bit gates can be realized by applying a resonant microwave pulse to the target qubit. The interaction between the microwave and the coupled qubits can be written as $V(x_1, x_2, t) = m\omega_{LC}^2 [(x_2 - x_{e2}) + \kappa(x_1 - x_{e1}) + x_m/2]x_m$, where $x_m(t) = x_{m0} \cos(\omega t)$ is the magnetic flux (normalized to Φ_0) coupled to the target qubit from the microwave with amplitude x_{m0} and frequency ω . For the CNOT gate, a π -pulse with $\omega = \Delta E_{34}/\hbar$, where $\Delta E_{34} = |E_4 - E_3|$, is used. Populations of the states $|10\rangle$ and $|11\rangle$ are exchanged after the π -pulse only if the initial state is $|10\rangle$ or $|11\rangle$ or a linear combination of them. Note that in this case in addition to the non-computational states, the undesired states also include the computational states $|00\rangle$ and $|01\rangle$. Using Eq. (1) and following the steps described above, the leakage of the CNOT gate $\eta = \max(\eta_{|00\rangle}, \eta_{|01\rangle}, \eta_{|10\rangle}, \eta_{|11\rangle})$ is calculated. In the calculations, up to 3-photon processes are included. The N -photon processes for $N > 3$ have negligible effects. For the SQUID qubits with the previously given DPs, the leakage is a function of WPs x_{e1} , x_{e2} , and κ . In Fig. 2(a) we plot the leakage of the CNOT gate versus x_{e2} and κ for $x_{e1} = 0.499$ and $x_{m0} = 2 \times 10^{-4}$. It is shown that the leakage of the CNOT gate is much smaller when the coupled SQUID qubits are operated around $x_{e2} = 0.4997$ and $\kappa = 7.5 \times 10^{-4}$ for $x_{e1} = 0.499$.

To evaluate the results obtained from ITA, we performed an accurate dynamic calculation by solving the TDSE of the coupled qubits $i\partial c_n(\tau)/\partial\tau =$

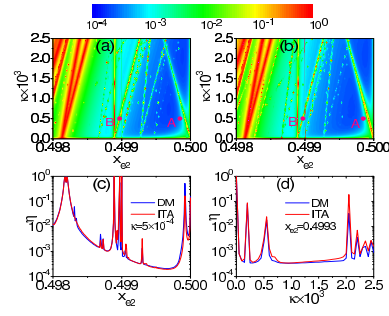


FIG. 2: Leakage of the CNOT gate for $x_{e1} = 0.499$ and $x_{m0} = 2 \times 10^{-4}$. (a) the leakage vs. x_{e2} and κ obtained from ITA, (b) the leakage vs. x_{e2} and κ obtained from DM, (c) comparison of the leakage vs. x_{e2} at $\kappa = 5 \times 10^{-4}$, and (d) comparison of the leakage vs. κ at $x_{e2} = 0.4993$.

$\sum_{n'} H_{nn'}^R(\tau) c_{n'}(\tau)$ for the probability amplitudes c_n of the first 20 eigenstates $|n\rangle$ using the split-operator method [29], where $\tau = \omega_{LC}t$ and $H_{nn'}^R = [E_n \delta_{nn'} + (n|V|n')]/\hbar\omega_{LC}$ [25]. The probability of being in the state $|n\rangle$ is $|c_n|^2$, from which the maximum probabilities on the undesired states and the leakage $\eta(x_{e1}, x_{e2}, \kappa)$ of the CNOT gate are calculated. The results are shown in Fig. 2(b) with the color scale identical to Fig. 2(a). To have a more quantitative comparison, we also plot, in Fig. 2(c) and (d), two line-cut figures at places with the richest structures in Fig. 2(a) and (b). The good agreement between the results of ITA and DM demonstrates the validity of using ITA to minimize the CNOT gate leakage.

One of the advantages of ITA is that it provides clear physical intuition and insight into the origin of intrinsic gate errors and thus how to reduce the problem by selecting appropriate WPs. Furthermore, ITA is orders of magnitude faster than DM. For instance, the result shown in Fig. 2(a) took less than 3 hours to compute on a dual-2.8 GHz processor Dell PRECISION 650 workstation while that shown in Fig. 2(b) took more than 300 hours on the same computer. Denoting τ_S and τ_T respectively the time needed to calculate the spectroscopic properties of an n -bit gate and that used to compute the probability evolution in DM for each component. The total times needed to compute the leakage by ITA and DM are approximately $\tau_I \approx \tau_S$ and $\tau_D \approx \tau_S + 2^n \tau_T$, respectively, where the factor 2^n is the number of components for the n -bit gate. Hence, $\tau_S < \tau_T$ and the ratio $\tau_D/\tau_I \approx 2^n \zeta$ increases exponentially with n , where $\zeta \equiv \tau_T/\tau_S$. For weak fields, $\zeta \gg 1$ and the ratio τ_D/τ_I is very large. For example, for the CNOT gate above $\zeta \sim 25$ and $\tau_D/\tau_I \sim 100$. Thus as the number of qubits increases the optimization of WPs of multi-bit quantum gates could become an intractable problem using DM.

To demonstrate quantitatively the effect of different WPs on intrinsic gate errors, we plot in Fig. 3(a) and (b) the population evolution of the computational states

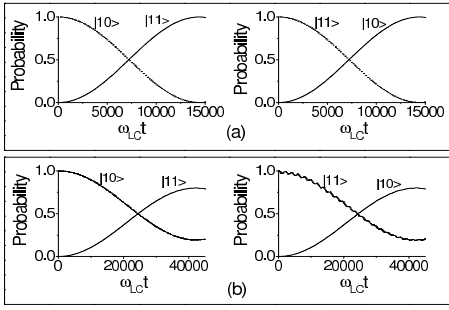


FIG. 3: Population evolution of the computational states $|10\rangle$ and $|11\rangle$ for the CNOT gates with different WPs: (a) $x_{e2} = 0.49985$ and $\kappa = 5 \times 10^{-4}$ corresponding to the point "A" in Fig. 2(a) [also (b)], and (b) $x_{e2} = 0.49897$ and $\kappa = 5 \times 10^{-4}$ corresponding to the point "B" in Fig. 2(a) [also (b)]. In both cases, $x_{m0} = 2 \times 10^{-4}$ and $x_{e1} = 0.499$.

$|10\rangle$ and $|11\rangle$ for the CNOT gate operated with two different sets of WPs corresponding to points "A" and "B" marked in Fig. 2(a) [also (b)], respectively. It is clearly shown that inversion from the initial state $|10\rangle$ ($|11\rangle$) to the final state $|11\rangle$ ($|10\rangle$) after the π -pulse is almost complete when operated at the point "A" but significantly incomplete at the point "B". We also computed the population evolution of the coupled qubits with the initial states $|00\rangle$ and $|01\rangle$ using the same microwave pulse. The system essentially stayed in the initial states for the gate operated at the point "A" but leaked significantly to the non-computational states for the gate at the point "B". The quality of a gate can be described by gate fidelity $F \equiv \text{Trace}[\rho_P \rho_I]$, where ρ_P and ρ_I are the physical and ideal density matrices after gate operation and the overline denotes averaging over all possible initial states [30]. For the CNOT gates operated at the point "A" we obtain $F_A = 0.9997$ which is very close to the ideal CNOT gate. In contrast, the gate operated at the point "B" has $F_B = 0.8061$ which is too large to be tolerated. Furthermore, at the point "A" the gate is about a factor of three faster than that at the point "B".

In summary, a very efficient method is proposed to optimize the WPs of microwave-driven quantum logical gates in multi-level qubits based on ITA. In this method, the leakage is estimated accurately from the spectroscopic properties of the qubits and minimized by choosing appropriate WPs. This method is exemplified by optimizing the WPs of coupled rf SQUID flux qubits for minimal leakage of the CNOT gate. The result is in good agreement with that obtained from dynamic calculations. Compared to the conventional dynamic method the ITA not only provides physical insight into the origin of gate leakage but also reduces the computational time by more than two orders of magnitude for the CNOT gate. Furthermore, since the ratio of the speed of ITA to that of DM scales exponentially as 2^n the ITA is scalable as the

number of qubit n increases. Our calculation also shows that high intrinsic fidelity CNOT gate can be achieved using microwave-driven rf SQUID qubits with properly selected WPs. Although the proposed ITA is only applied, as an example, to the rf SQUID qubits, it is also valid for other microwave-driven multi-level qubits. Therefore, ITA provides a much needed solution for the optimization of WPs of multi-bit gates implemented with multi-level physical qubits, for which DM is extremely time consuming or could even become intractable.

This work was supported in part by the NSF (DMR-0325551) and AFOSR, NSA and ARDA through DURINT grant (F49620-01-1-0439).

-
- [1] J. I. Cirac and P. Zoller, Phys. Rev. Lett. **74**, 4091 (1995).
 - [2] C. Monroe et al., Science **272**, 1131 (1996).
 - [3] N. A. Gershenfeld and I. L. Chuang, Science **275**, 350 (1997).
 - [4] J. A. Jones, M. Mosca, and R. H. Hansen, Nature **393**, 344 (1998).
 - [5] Q. A. Turchette et al., Phys. Rev. Lett. **75**, 4710 (1995).
 - [6] M. Brune et al., Phys. Rev. Lett. **77**, 4887 (1996).
 - [7] J. E. Mooij et al., Science **285**, 1036 (1999).
 - [8] Y. Makhlin, G. Schon, and A. Shnirman, Rev. Mod. Phys. **73**, 357 (2001).
 - [9] Y. Nakamura, Y. A. Pashkin, and J. S. Tsai, Nature **398**, 786 (1999).
 - [10] D. Vion et al., Science **296**, 886 (2002).
 - [11] Y. Yu et al., Science **296**, 889 (2002).
 - [12] J. M. Martinis et al., Phys. Rev. Lett. **89**, 117901 (2002).
 - [13] I. Chiorescu et al., Science **299**, 1869 (2003).
 - [14] Y. A. Pashkin et al., Nature **421**, 823 (2003).
 - [15] T. Yamamoto et al., Nature **425**, 941 (2003).
 - [16] A. J. Berkley et al., Science **300**, 1548 (2003).
 - [17] I. Chiorescu et al., Nature **431**, 159 (2004).
 - [18] J. B. Majer et al., Phys. Rev. Lett. **94**, 090501 (2005).
 - [19] R. Fazio, G. M. Palma, and J. Siewert, Phys. Rev. Lett. **83**, 5385 (1999).
 - [20] Z. Zhou, S.-I. Chu, and S. Han, Phys. Rev. B **66**, 054527 (2002).
 - [21] Z. Zhou, S.-I. Chu, and S. Han, Phys. Rev. B **70**, 094513 (2004).
 - [22] M. A. Kmetz, R. A. Thuraishingham, and W. J. Meath, Phys. Rev. A **33**, 1688 (1986).
 - [23] B. W. Shore, *The theory of coherent atomic excitation*, vol. 1 (John Wiley and Sons, New York, 1990).
 - [24] V. V. Danilov, K. Likharev, and A. B. Zorin, IEEE Trans. Magn. **19**, 572 (1983).
 - [25] Z. Zhou, S.-I. Chu, and S. Han, IEEE Trans. Appl. Supercon. (2005, in press).
 - [26] S.-I. Chu, Chem. Phys. Lett. **167**, 155 (1990).
 - [27] T. V. Filippov et al., IEEE Trans. Appl. Supercon. **13**, 1005 (2003).
 - [28] A. M. van den Brink and A. J. Berkley, cond-mat/0501148 (unpublished).
 - [29] M. R. Hermann and J. A. Fleck, Jr., Phys. Rev. A **38**, 6000 (1988).
 - [30] X. Li et al., Science **301**, 809 (2003).